American Journal of Nano Research and Applications
2026, Vol. 14, No. 2, pp. 16–27
https://doi.org/10.11648/j.nano.20261402.11

Research Article

Synthesis of Ag: 4-Aminophenol: Cyclodextrin Nanomaterials and 4AP: CD Inclusion Complexation at Different pH

Narayanasamy Rajendiran[1, *], Ayyadurai Mani[1], Palanichamy Ramasamy[2], Sengamalai Senthilmurugan[3]

[1]Department of Chemistry, Annamalai University, Annamalai Nagar, India
[2]Molecular Biophysics Unit, Indian Institute of Science, Bangalore, India
[3]Department of Zoology, Annamalai University, Annamalai Nagar, India

Abstract

Inclusion complexation of 4-aminophenol (4AP) with α-CD and β-CD at pH ~2, pH ~7, and pH ~11 was investigated using UV-visible, steady-state and time-resolved fluorescence measurements, along with molecular modeling studies. Ag: 4AP: CD nanomaterials were synthesized and characterized by SEM, DSC, FTIR, XRD, and ^{1}H NMR analyses. Increasing CD concentrations induced dual emission in the excited state. The changes in emission intensity at pH ~7 and the structured emission observed at pH ~11 indicate the formation of excimers in the excited state, while ground-state dimers are not formed due to the ionization of amino and hydroxyl groups. The lifetimes of the inclusion complexes were longer than that of the free 4AP molecule. The geometrical restriction of the α-CD cavity likely limits the free rotation of the amino and hydroxyl groups, thereby enhancing the intensity of the IPT emission. The calculated HOMO-LUMO energy gap, total energy, free energy, enthalpy, entropy, dipole moment, and zero-point vibrational energy of the CD: 4AP complex differed significantly from those of the isolated 4AP, α-CD and β-CD molecules, and both the vertical and horizontal bond lengths between the amino and hydroxy groups are smaller than the β-CD cavity size confirming the formation of an inclusion complex. SEM-EDX analysis confirmed the presence of 40.4% carbon, 50.4% oxygen, and 9.2% silver in the nanomaterials. DSC, FTIR, XRD, and ^{1}H NMR results collectively support the successful formation of Ag: 4AP: CD nanomaterials.

Keywords

4-aminophenol, Cyclodextrin, Silver Nano, pH Effects, Excimer

1. Introduction

The fluorescence characteristics of many organic molecules are highly sensitive to their surrounding environment. Microheterogeneous systems [1-5] can significantly influence these photophysical properties, enabling such mole-

*Correspondence: Narayanasamy Rajendiran (drrajendiran1967@gmail.com)

Received: 11 March 2026; **Accepted:** 23 March 2026; **Published:** 10 April 2026

cules to serve as effective probes for investigating microheterogeneous media [6-10]. Although numerous host-guest systems form inclusion complexes with cyclodextrins (CDs), the resulting photophysical changes are often too small to yield meaningful information on CD microheterogeneity or probe location [11-15].

Since several organic molecules [16-20] exhibit remarkable sensitivity to pH and microenvironmental changes, it is worthwhile to examine substituted phenols under various conditions [21-25]. In this context, we report: (i) the absorption and fluorescence spectral shifts and first excited singlet-state lifetimes of 4-aminophenol (4AP) in α-CD, β-CD, solvents of different polarities, and various pH conditions; (ii) the proton transfer behavior of 4AP in aqueous, α-CD, and β-CD media; (iii) the structures and geometries of the resulting inclusion complexes using PM3 molecular modeling; and (iv) the doping effects of 4AP: CD on silver nanomaterials, characterized by DSC, FTIR, ^{1}H NMR, and SEM analyses [26-30].

2. Materials and Methods

2.1. Preparation of CD Solution

A 4AP stock solution (2×10^{-2} mol/dm^3) was prepared, and aliquots of 0.1 or 0.2 mL were transferred into 10 mL volumetric flasks. Varying concentrations of α-CD or β-CD (0.2, 0.4, 0.6, 0.8, and 1.0×10^{-2} mol/dm^3) were added, followed by dilution to 10 mL with triple-distilled water. The mixtures were shaken thoroughly, yielding a final 4AP concentration of 4×10^{-4} mol/dm^3 in all samples. Experiments were conducted at 298 K.

2.2. Preparation of Ag: 4AP: CD Nanomaterials

A 0.01 M silver nitrate solution was prepared in 50 mL of deionized water and warmed to 50-60 ℃ for 30 minutes. To this, 1-2 mL of 1% trisodium citrate solution (1 g in 100 mL deionized water) was added with vigorous stirring. The appearance of a pale yellow color indicated the formation of silver nanoparticles [26-30].

Cyclodextrin (1 mmol) was dissolved in 40 mL distilled water, and 4AP (1 mmol) dissolved in 10 mL ethanol was added slowly with continuous stirring at 50 ℃ for 2 hours. The silver nanoparticle solution was then introduced, and stirring continued for another 2 hours. The resulting mixture was gently heated to 40-50 ℃ until its volume decreased by about 50%. The solution was refrigerated overnight at 5 ℃, leading to the precipitation of Ag-4AP-CD nanomaterials. The solid product was collected by filtration, washed with small amounts of ethanol and water to remove uncomplexed components, dried under vacuum at room temperature, and stored in an airtight container. The obtained powder samples were used for further characterizations [26-30].

3. Results and Discussion

3.1. Effect of α-CD and β-CD with pH on 4-aminophenol

The absorption and fluorescence maxima of 4-aminophenol (4AP) in pH~2, pH~7, and pH~11 buffer solutions containing various concentrations of α-CD and β-CD are presented in Table 1, Figure 1, and Figure 2. In pH~7 buffer, 4AP predominantly exists as the hydroxyl monoanion; therefore, the inclusion behavior of the neutral, monocationic, and monoanionic species was investigated in pH~2, pH~7, and pH~11 solutions, respectively. In the absence of CDs, the absorption and emission maxima of 4AP appear at the following wavelengths: pH~2: λ_{abs} = 272, 218 nm; λ_{flu} = 366, 325 nm, pH~7: λ_{abs} = 298, 230 nm; λ_{flu} = 370, 312 nm, pH~11: λ_{abs} = 333, 253 nm; λ_{flu} = 365, 312 nm. These results confirm that the monocationic, neutral, and hydroxyl monoanionic forms are predominant at pH~2, pH~7, and pH~11, respectively. At pH~7, the absorption (298, 230 nm) and emission (370 nm) bands closely resemble those observed in non-aqueous solvents, supporting the assignment to the molecular (neutral) form of 4AP.

The data further show that the absorption spectrum of 4AP in water at pH~7 exhibits a blue shift (298, 230 nm), while the emission band is red-shifted (370 nm) compared with other solvents. In acidic medium (pH~2), the absorption bands undergo a blue shift (272, 218 nm), whereas basic medium (pH~11) causes a red shift (333, 253 nm). The blue shift at pH~2 is attributed to protonation of the amino group (formation of the monocation), while the red shift at pH~11 arises from deprotonation of the phenolic OH group (formation of the monoanion). These observations are consistent with the known spectroscopic characteristics of amino and hydroxyl functionalities [16-30].

In the ground state, increasing the concentrations of α-CD and β-CD produced the following effects in 4AP:

a) pH ~2: The absorbance increased in both α-CD and β-CD, and no significant spectral shift was observed in either aqueous or CD-containing solutions (λ_abs ≈ 272, 218 nm).

b) pH ~7: In α-CD, the absorbance increased with no appreciable spectral shift (λ_abs ≈ 298, 230 nm). In β-CD, however, the absorbance at 298 nm decreased while a new band emerged and intensified at 272 nm. A pronounced blue shift occurred in β-CD (from 298, 230 nm to 272, 218 nm), and the hypsochromic maxima correspond to those observed in pH ~2 medium.

c) pH ~11: In α-CD, a slight increase in absorbance was observed without any shift in wavelength (λ_abs ≈ 333, 253 nm). In β-CD, the absorption maxima underwent a blue shift (from 333, 253 nm to 296, 231 nm). Additionally, the absorbance at 333 nm decreased while that at 298 nm increased. The hypsochromic maxima resemble those of CD-free aqueous pH ~7 medium.

In the excited state, increasing α-CD and β-CD concentrations yielded the following observations:

a) pH ~2: The emission intensity increased in α-CD but decreased in β-CD. In water and α-CD media, no significant shift occurred at 366 nm, although a slight blue shift appeared at shorter wavelengths (325 → 320 nm). In β-CD, a small red shift occurred at 366 → 370 nm, accompanied by a marginal hypsochromic shift at shorter wavelengths (325 → 312 nm). Interestingly, in both CDs, the intensity at 440 nm increased slightly with concentration, despite no new emission band appearing.

Table 1. *Absorption and fluorescence maxima of 4-Aminophenol (4AP) with different α-CD and β-CD concentrations.*

Concentration of α-CD x10^{-3} M	pH - 2.0				pH - 7				pH - 11			
	λ_{abs}	log ε	λ_{flu}	Life time	λ_{abs}	log ε	λ_{flu}	Life time	λ_{abs}	log ε	λ_{flu}	Life time
4AP only (in water)	272 218	3.36	366 325	0.37	298 230	3.33	370 312	0.41	333 253	3.08	440 365 312	0.21
0.2 M α-CD	272 218	3.37	366 320	0.41	297 229	3.35	369 312	0.52	333 253	3.10	440 365 312	0.24
1.0 M α-CD	272 218	3.48	366 320	0.54 0.14	297 230	3.48	370 313	0.61 0.18	333 253	3.19	440 365 312	0.27 0.15
0.2 M β-CD	272 218	3.21	370 325	0.48	296 223	3.29	368 325	0.59	333 253	3.36	365 312sh	0.25
1.0 M β-CD	272 218	3.29	370 312	0.59 0.18	272 218	3.04	367 312	0.65 0.21	296 231	3.10	365 312sh	0.30 0.18
K (1: 1) x10^5 M^{-1} α-CD	36.6		235		58.4		270		56.0		291	
ΔG (kcalmol^{-1}) α-CD	-9.1		-13.7		-10.2		-14.1		-10.1		-14.2	
K (1: 1) x10^5 M^{-1} β-CD	128.1		352		119.0		325		117.0		318	
ΔG (kcalmol^{-1}) β-CD	-12.2		-14.7		-12.0		-14.5		-11.9		-14.5	
Excitation wavelength (nm)			280				280				280	

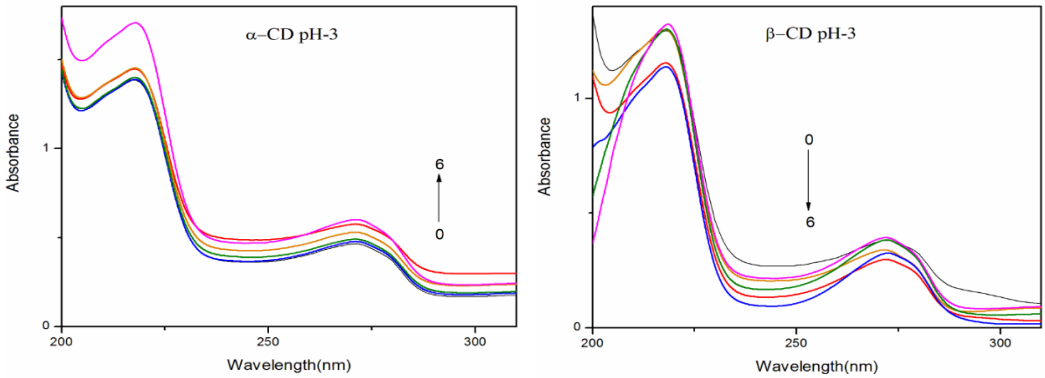

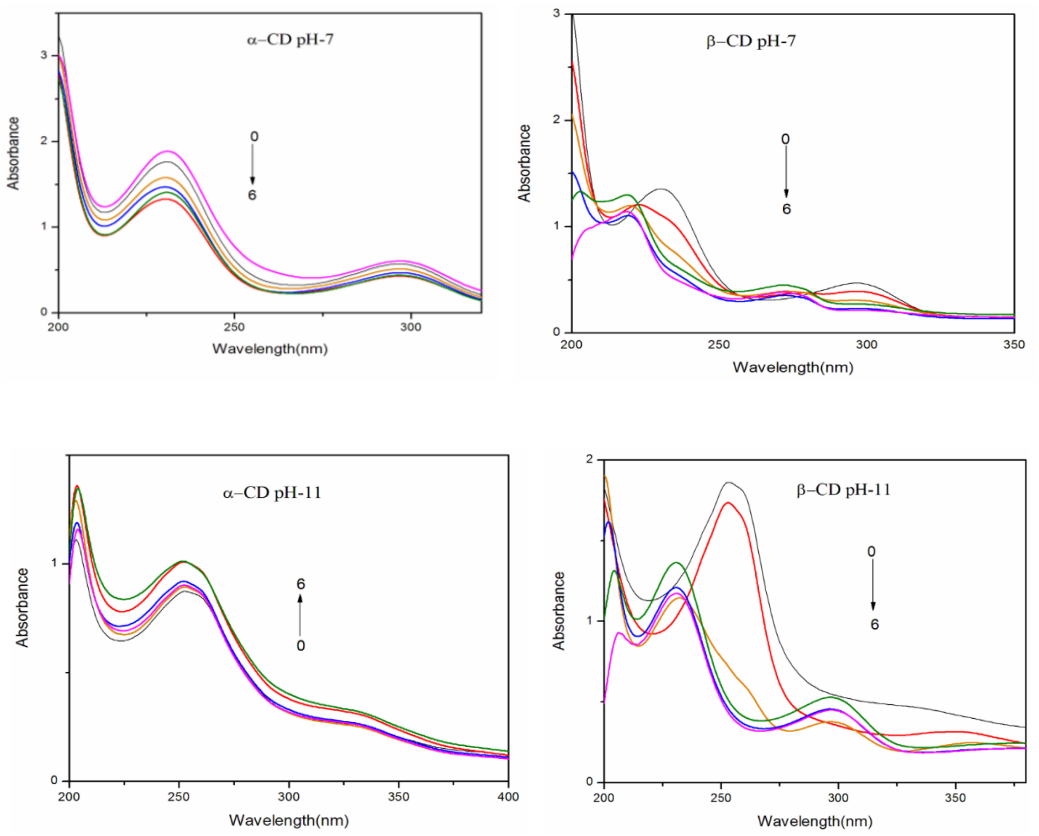

Figure 1. *Absorbance spectra of 4AP in different α-CD and β-CD concentrations (M): (1) 0, (2) 0.002, (3) 0.004, (4) 0.006, (5) 0.008 and (6) 0.01.*

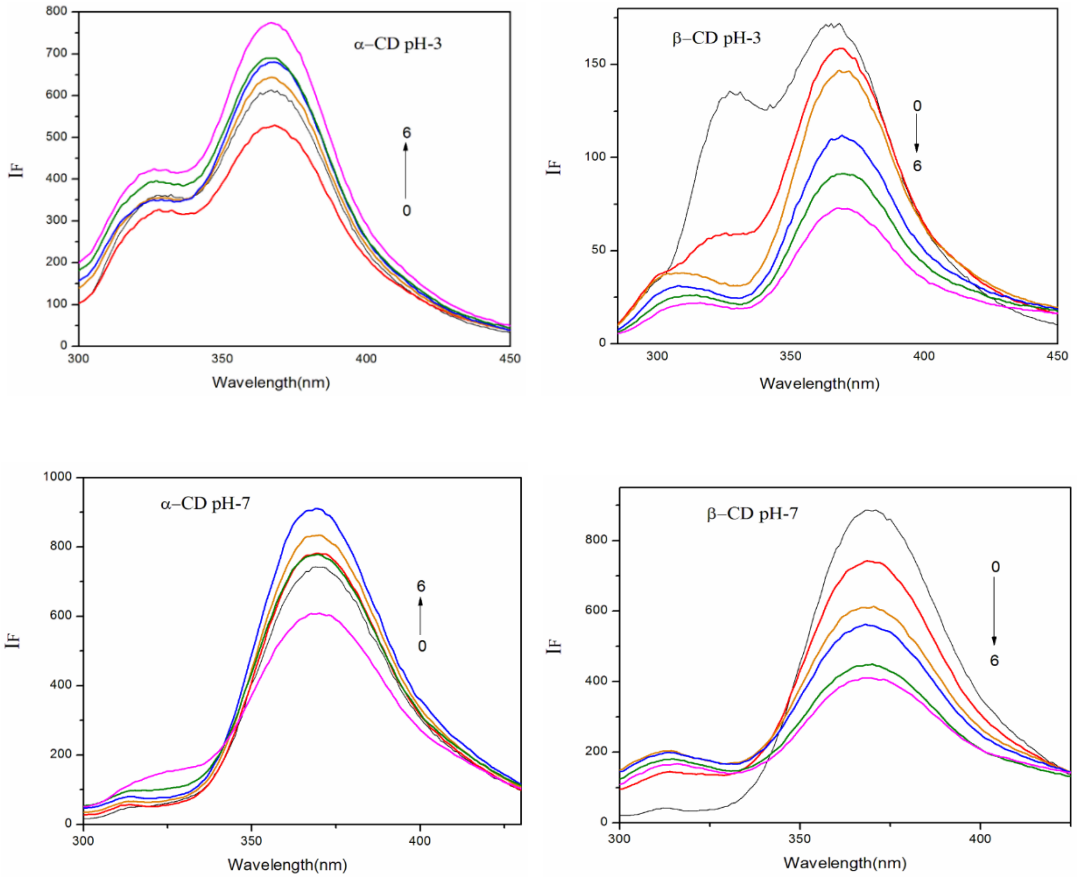

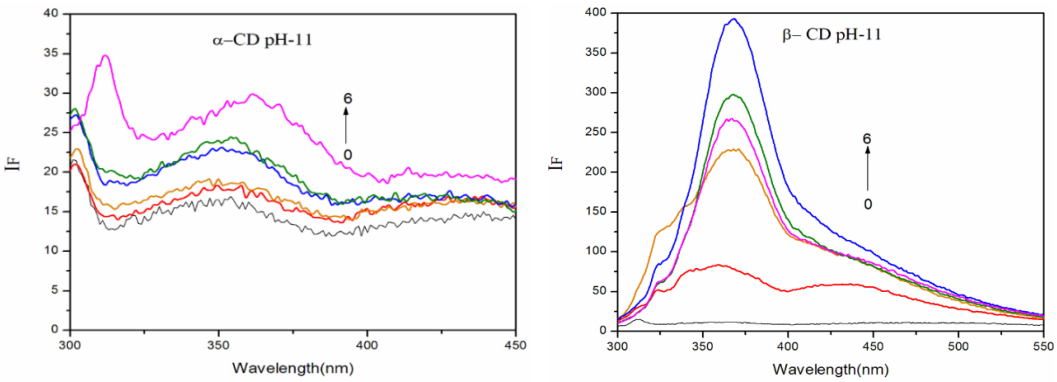

Figure 2. *Fluorescence spectra of 4AP in different α-CD and β-CD concentrations (M): (1) 0, (2) 0.002, (3) 0.004, (4) 0.006, (5) 0.008 and (6) 0.01.*

b) pH ~7: In α-CD, the emission intensity increased at the same wavelengths (370, 312 nm). In β-CD, the intensity at 370 nm decreased, while intensities at 325 and 440 nm increased. A blue shift was also observed (370, 325 nm → 367, 312 nm). Similar to pH ~2, the 440-nm band increased slightly with CD concentration without the appearance of a new emission maximum.

c) pH ~11: Three emission maxima (440, 365, 325 nm) were observed in water and α-CD solutions, whereas the longest-wavelength band (440 nm) was absent in β-CD. In both CDs, the intensities of all present bands increased without wavelength shifts. Overall, emission intensities at pH ~11 were much weaker than at other pH conditions, consistent with the reduced fluorescence of the monoanionic form of 4AP.

In pH ~2 and pH ~7, the absorption maxima remain nearly identical at higher β-CD concentrations. At pH ~11, the absorption maximum at elevated β-CD levels corresponds closely to that of the CD-free aqueous pH ~7 solution. Smooth emission profiles were observed in both CD media at pH ~2 and pH ~7, whereas well-resolved, structured emission bands appeared at pH ~11. The distinct spectral shifts in both absorption and fluorescence across the different pH conditions clearly demonstrate that 4AP forms multiple types of inclusion complexes with CDs [16-30].

The presence of an isosbestic point in absorption spectra typically signifies the formation of a well-defined 1: 1 complex. In all three pH conditions, however, the absence of an isosbestic point, together with the dissimilar spectral shifts, indicates the formation of different types of 4AP-CD inclusion complexes. The binding constants and stoichiometry of these complexes were evaluated using the Benesi-Hildebrand equation. The negative ΔG values (Table 1) confirm that the inclusion process is spontaneous at 303 K and exothermic in nature.

Variations in emission intensities at pH ~2 and pH ~7 and the structured emission observed at pH ~11 suggest the potential formation of excimers in the excited state, likely stabilized through hydrogen bonding. Such dimer formation does not occur in the ground state because the amino and hydroxyl groups are ionized. Nonetheless, the observed increase in emission intensities at 325 nm and 440 nm, along with a decrease at 365 nm upon increasing CD concentrations, indicates that excimer formation may occur in pH ~2 and pH ~7 media.

As noted earlier, the emission intensity increases significantly with rising α-CD concentration, whereas it decreases with higher β-CD concentration. In β-CD, the hypsochromic shifts observed at pH ~7 and pH ~11 imply protonation of the amino and hydroxyl groups, respectively. This behavior arises because the CD rims, rich in secondary hydroxyl groups, create a microenvironment comparable to that of polyhydroxy alcohols [16-30]. Consequently, the emission characteristics of 4AP vary distinctly across pH ~2, pH ~7, and pH ~11 in CD-containing media.

The higher binding constants and the observed blue shifts at pH ~2 and pH ~7 indicate that the 4AP molecule is fully encapsulated within the CD cavities. Moreover, 4AP is more deeply embedded in the hydrophobic interior of β-CD than in α-CD. This difference arises from the geometric constraints of the CD cavities: although both CDs share the same height (7.8 Å), α-CD has a smaller internal cavity diameter (4.7-5.3 Å) compared to β-CD (6.0-6.5 Å). The vertical (6.34 Å) and horizontal (4.30 Å) distances between the -NH_2 and -OH groups of 4AP are within the accessible dimensions of the CD cavities, and all other intramolecular bond distances are even shorter. The systematic increase and decrease in emission intensities with rising concentrations of α-CD and β-CD, respectively, support this interpretation. Thus, the distinct spectral changes observed upon CD addition at various pH values suggest that the geometry of the inclusion complexes varies, particularly in terms of the orientation of 4AP within the cavity.

3.2. Excimer Emission

The broad emission bands detected in CD-containing solutions indicate that 4AP may form 1: 2 inclusion complexes with CDs, wherein two 4AP molecules occupy a single CD cavity [36-38]. As the CD concentration increases, the intensity of the longer-wavelength (LW) band increases slightly, accompanied by noticeable band broadening. Concurrently,

the intensity of the middle-wavelength (MW) fluorescence decreases, and the shorter-wavelength (SW) band undergoes a blue shift. This broad emission is characteristic of excimer fluorescence from 4AP. The excimer emission may originate from either 1: 2 or 2: 1 CD: 4AP complexes formed through the self-association of 1: 1 CD-4AP inclusion complexes [36-38]. At pH ~11, the excimer emission is considerably weaker than at pH ~2 and pH ~7.

No excimer fluorescence is observed when a dilute 4AP solution (2×10^{-6} M) containing CDs is excited, indicating that excimer formation requires higher 4AP concentrations and likely arises from self-association of 1: 1 CD-4AP complexes. This explains the observed variations enhancement or reduction of MW and LW emission intensities in the presence of CDs. To identify the type of excimer complex formed (CD_2: 4AP vs. CD: $(4AP)_2$), the concentration dependence of the excimer fluorescence was analyzed. The calculated curves accurately reproduced the experimental fluorescence-concentration profiles, clearly demonstrating that the excimer emission originates from 1: 2 inclusion complexes of the form CD-$(4AP)_2$.

The plot (figure not shown) displays an upward-curving (concave) trend and the absence of an isosbestic point in the absorption spectra, indicating the presence of inclusion complexes other than the simple 1: 1 type in aqueous 4AP-CD systems. Because the α-CD cavity is not sufficiently large to completely encapsulate a 4AP molecule, a portion of the guest is likely to protrude from the α-CD cavity. Furthermore, due to the restricted internal space of α-CD, the guest molecule cannot adopt a sandwich-type arrangement. As a result, an additional α-CD molecule may associate with the initial 1: 1 complex, leading to the formation of $(\alpha\text{-CD})_2$-(4AP), α-CD-$(4AP)_2$, or $[(\alpha\text{-CD})_2\text{-}(4AP)_2]$ complexes. The pronounced enhancement in fluorescence intensity and the sharpening of vibronic bands with increasing α-CD concentration support the formation of 1: 2 [α-CD-$(4AP)_2$] inclusion complexes.

The excimer-emitting species was further identified using an established method [31-33]. Above the pK_a of the $-CH_2OH$ groups of CDs, a 2: 2 inclusion complex is expected to dissociate into two 1: 1 complex due to electrostatic repulsion between the negatively charged secondary hydroxyl groups. If the excimer originated from a 2: 2 complex, a sharp decrease in excimer intensity would be expected above this pK_a. Conversely, if the excimer emission arises from a 1: 2 [CD: $(4AP)_2$] complex, the excimer intensity should show little or no pH dependence. To test this, the pH dependence of the excimer emission was examined for 4AP in CD solution (1.0×10^{-2} M). The excimer fluorescence intensity at pH ~11 was significantly lower than at pH ~2 and pH ~7, indicating that the excimer emission does not arise from a 2: 2 complex in β-CD. The absence of isosbestic points in the absorption spectra (Figures 1 and 2) further supports the lack of 2: 2 inclusion complexes.

To further substantiate excimer formation between 4AP and α-/β-CD, solvent-induced changes in the absorption and fluorescence spectra were analyzed. The spectral maxima of 4AP in various solvents are as follows: Cyclohexane: λ_abs ≈ 303, 235 nm; λ_flu ≈ 344 nm, Acetonitrile: λ_abs ≈ 310, 240 nm; λ_flu ≈ 364 nm, Methanol: λ_abs ≈ 303, 237 nm; λ_flu ≈ 364 nm, Water: λ_abs ≈ 297, 230 nm; λ_flu ≈ 370 nm.

Comparison with aniline (cyclohexane: λ_{abs} ~283, 235 nm, λ_{flu}~320 nm; acetonitrile: λ_{abs}~286, 238 nm, λ_{flu}~329; methanol: λ_{abs} ~284, 232 nm, λ_{flu} ~ 334; water: λ_{abs} ~278, 230 nm, λ_{flu} ~335 nm) [34-36] and phenol (cyclohexane: λ_{abs} ~277-271 nm, λ_{flu}~300 nm; acetonitrile: λ_{abs}~278-272 nm, λ_{flu}~302; methanol: λ_{abs} ~275-272 nm, λ_{flu} ~ 305; water: λ_{abs}~272-278 nm, λ_{flu}~305) [34-36] the absorption maxima of 4AP are consistently red-shifted in all solvents, indicating electronic delocalization between its amino and hydroxyl groups. Across the solvent series, the absorption maxima of 4AP shift to longer wavelengths from cyclohexane to acetonitrile but undergo a blue shift in alcohols and water, while the emission maxima systematically red-shift from cyclohexane to water. In all solvents, 4AP exhibits a single broad fluorescence band, and the absence of a long-wavelength emission band in polar solvents confirms that excimer or exciplex formation does not occur in solution.

3.3. Excited State Lifetime Measurements

Table 1 presents the average lifetimes of 4AP in α-CD and β-CD media. In aqueous solution, the excimer emission of 4AP exhibits a very short decay time, which is noticeably altered upon the addition of CDs. The lifetime of 4AP in water is lower than that in CD-containing media. With increasing CD concentration, the excimer decay component rises markedly, indicating that encapsulation within the CD cavity stabilizes the excited state. The lifetime of 4AP increases in the order: water < α-CD < β-CD, suggesting that the β-CD: 4AP inclusion complex is more stable than the corresponding α-CD complex. The observed increase in τ values with increasing CD concentration arises from the confinement of 4AP within the CD cavities. The τ_1 and τ_2 components depend on the type of CD and the processes associated with short-lived excited species, likely due to restricted vibrational relaxation of 4AP in the excited state.

The enhancement in lifetime upon complexation reflects the degree of confinement experienced by 4AP. The larger cavity of β-CD allows deeper encapsulation and stronger guest-host interactions compared with α-CD. Consequently, the longer lifetime is attributed to a deeply included guest species, whereas the shorter lifetime corresponds to a more weakly associated form. Because β-CD can accommodate 4AP more fully than α-CD, a greater increase in fluorescence lifetime is observed in β-CD. The fluorescence decay monitored at 365 nm varies significantly with CD concentration, confirming that 4AP forms excimers in the presence of CDs. Additionally, the excimer decay component is longer-lived than the monomer emission.

3.4. Molecular Modeling

The structures of 4AP, α-CD, and β-CD were optimized using the PM3 method (Figure 3), and the resulting thermodynamic parameters are summarized in Table 2. The semiempirical calculations indicate the absence of charge-transfer interactions between guest and host, which is further supported by the zero Mulliken charges for the complexes. The thermodynamic parameters (ΔE, ΔG, and ΔH) show that complexation between 4AP and CDs is predominantly enthalpically favorable. The interior cavity diameters of α-CD and β-CD are 4.7-5.3 Å and 6.0-6.5 Å, respectively, while the exterior cavity size of both CDs is approximately 7.8 Å. For 4AP, the vertical and horizontal distances between the -NH_2 and -OH groups are 6.34 Å and 4.30 Å, respectively (Figure 3). As both dimensions fall within the cavity sizes of α-CD and β-CD, the 4AP molecule can be fully accommodated within either cavity. Upon inclusion, slight geometric changes occur in 4AP, notably in dihedral angles, suggesting that 4AP adopts a specific conformation to form a stable complex. The optimized structures of the CD: 4AP complexes clearly show the guest molecule positioned within the CD cavity. The negative ΔG values for complex formation confirm that the inclusion processes are spontaneous and exothermic at 303 K.

Table 2. *Thermodynamic parameters and HOMO-LUMO energy calculations for 4AP and its inclusion complexes by PM3 method.*

Properties	4AP	α-CD	β-CD	4AP: α-CD	4AP: β-CD
E_{HOMO} (eV)	-8.20	-10.37	-10.35	-7.73	-7.85
E_{LUMO} (eV)	0.06	1.26	1.23	0.43	0.48
E_{HOMO} - E_{LUMO} (eV)	-8.27	-11.63	-11.58	-7.30	-8.33
Dipole moment (D)	2.32	11.34	12.29	11.61	11.87
E*	-21.13	-1247.62	-1457.63	-1284.23	-1509.18
ΔE*				-15.48	-240.43
G*	49.80	-676.37	-789.52	-621.35	-704.56
ΔG*				-4.78	-4.84
H*	74.26	-570.84	-667.55	-476.51	-588.29
ΔH				-20.10	-8.46
S**	0.082	0.353	0.409	0.451	0.463
ΔS**				0.02	-0.04
ZPE*	67.67	635.09	740.56	710.63	796.52
Mullikan charge	0.00	0.00	0.00	0.00	0.00

*kcal/mol; **kcal/mol-Kelvin; ZPE = Zero point vibration energy

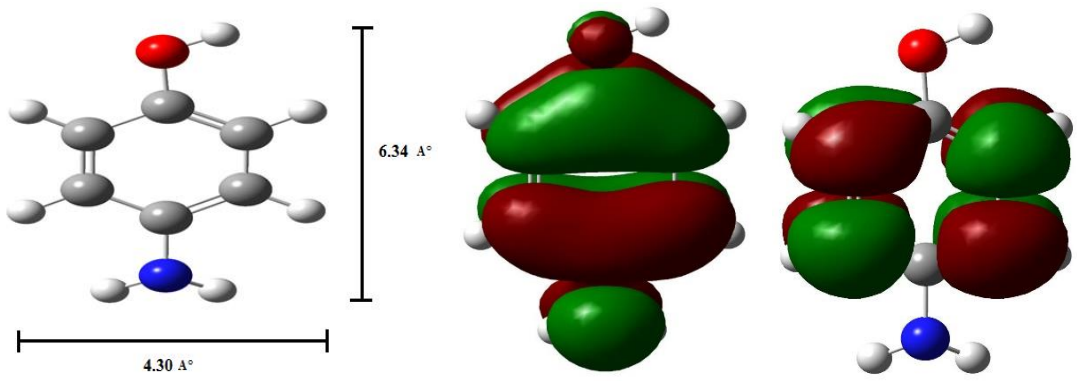

Figure 3. *PM3 optimized structures of (a, b) 4AP (c, d) HOMO, LUMO of 4AP.*

3.5. Nanomaterials Studies

3.5.1. Scanning Electron Microscopy

The morphologies of silver nanoparticles, 4AP, and the Ag: 4AP: α-CD and Ag: 4AP: β-CD nanomaterials were examined using SEM (Figure 4). The SEM images reveal clustered particle formations for Ag nanoparticles, a stone-like morphology for pure 4AP, a similar stone-like structure for Ag: 4AP: α-CD, and a distinct microrod-shaped morphology for Ag: 4AP: β-CD. These observations clearly highlight the morphological variations among silver nanoparticles, 4AP, and their corresponding nanomaterials. SEM-EDX analysis further confirms the presence of 40.4% carbon, 50.4% oxygen, and 9.2% silver in the nanomaterials. The distinct structural differences among pure Ag nanoparticles, 4AP, and the inclusion complexes strongly support the successful formation of the Ag: 4AP: CD nanomaterials.

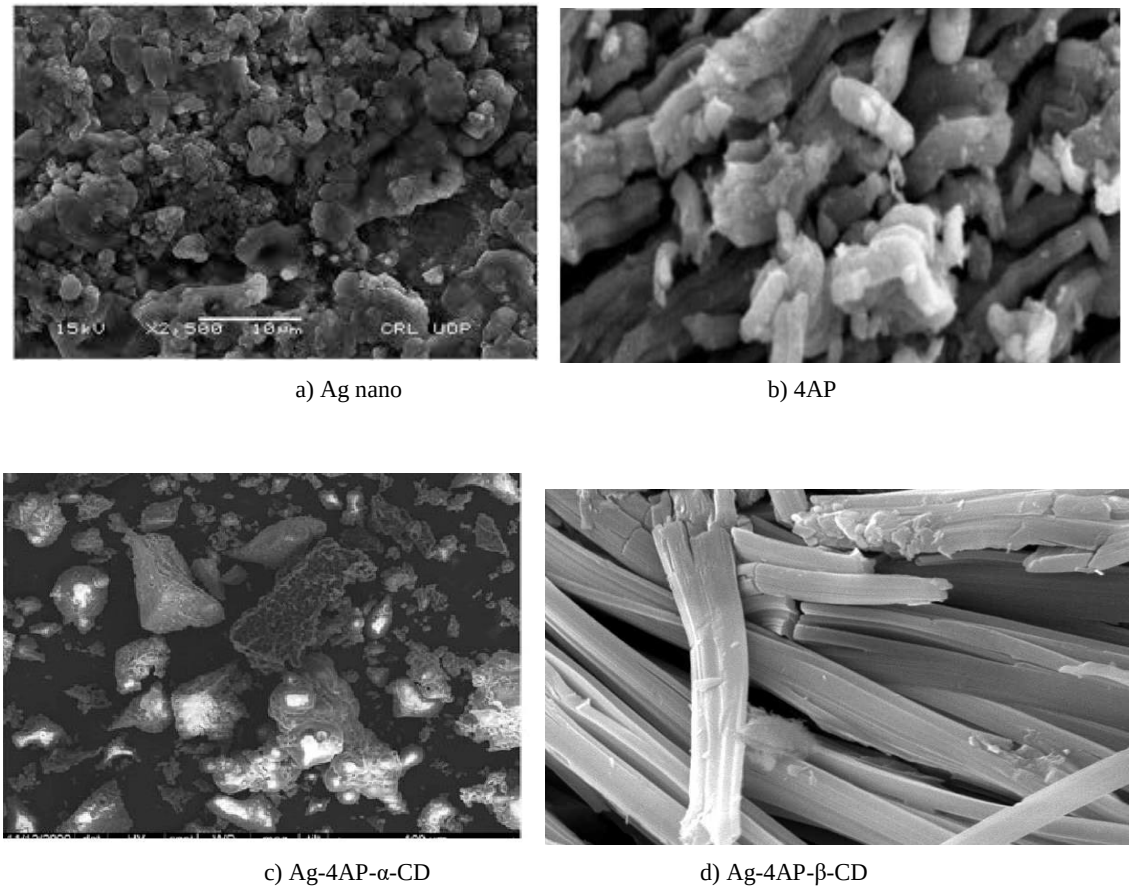

a) Ag nano b) 4AP

c) Ag-4AP-α-CD d) Ag-4AP-β-CD

Figure 4. *SEM images for a) Ag nano, b) 4AP, c) Ag-4AP-α-CD and d) Ag-4AP-β-CD.*

3.5.2. Differential Scanning Colorimeter

The DSC thermogram of α-CD displays three endothermic peaks at 79.2, 109.1, and 137.5°C, while β-CD exhibits a broad endothermic peak at 128.6 ℃. These thermal events correspond to the loss of crystallization water from the CDs [40-49]. Pure 4AP shows a sharp melting endotherm at 188 ℃. Broader endothermic signals observed for α-CD, β-CD, and their inclusion complexes arise from water loss associated with the CDs. Notably, the DSC profiles of the Ag-4AP-CD complexes do not display the characteristic peaks of free 4AP or CDs. Instead, new endothermic peaks are observed at 265°C for Ag: 4AP: α-CD and 287°C for Ag: 4AP: β-CD, confirming the formation of new nanomaterial phases.

3.5.3. Infrared Spectral Studies

In the spectrum of 4AP, the N-H, O-H, and C-H stretching vibrations appear at 3341, 3284, and 3033 cm^{-1}, respectively. The aromatic C=C stretch and the NH_3^+ antisymmetric vibration are observed at 1615 and 3180 cm^{-1}. Additional characteristic bands include aromatic C-C (1478 cm^{-1}), C-OH (1170 cm^{-1}), and C-O (1388 cm^{-1}) stretching modes. The C-O-C and C-N vibrations appear near 1256 and 1162 cm^{-1}. Aromatic ring deformation and O-H out-of-plane vibrations are observed at 524, 707, and 647 cm^{-1}.

In the nanomaterials, the NH_2 and O-H stretching bands shift to 3263 and 2906 cm^{-1}. The aromatic C=C, C-OH, and C-O stretching bands are recorded at 1625, 1015, and 1323

cm^{-1}, while the aromatic ring deformation appears at 569 cm^{-1}. A pronounced decrease in peak intensities in the Ag: 4AP: CD nanomaterials suggest strong interactions between 4AP and silver nanoparticles.

3.5.4. X RD Spectral Studies

The crystallinity of the nanoparticles was evaluated using XRD [40-49]. Pure silver nanoparticles exhibit strong reflections at 38.11 °, 44.30 °, 64.45 °, and 77.40 °, characteristic of the face-centered cubic structure of metallic silver. α-CD shows diffraction peaks near 11.94 °, 14.11 °, and 21.77 °, while β-CD displays peaks at 11.49 ° and 17.58 °, though intensities may vary depending on preparation conditions. The XRD pattern of 4AP corresponds to an orthorhombic crystal system with peaks at 24.1 °, 28.50 °, 36.21 °, 41.6 °, 45.8 °, 56.5 °, 61.8 °, 66.7°, and 71.7°. For the Ag/4AP: β-CD nanomaterials, distinct diffraction peaks are observed at 22.13 °, 29.26 °, 37.25 °, 41.76 °, 47.63 °, 55.86 °, 65.04 °, and 76.75 °. The significant changes in peak positions and intensities, compared with the individual components, confirm the formation of new nanomaterial phases.

3.5.5. ^{1}H NMR Spectral Studies

Ⱨ NMR spectra of 4AP and its inclusion complexes were recorded at 25 ℃ in DMSO-d_6 (Table 3). CDs contain six types of protons, and their chemical shift assignments are well established [37-39]. Among these, H-3 and H-5 protons lie inside the CD cavity and are particularly sensitive to guest inclusion; thus, their chemical shifts show noticeable changes in the complexes. Minor variations are observed for exterior protons (H-1, H-2, and H-4). Guest molecule protons typically exhibit significant chemical shift changes upon encapsulation within CD cavities. For the Ag-4AP-CD nanomaterials, the 4AP proton signals shift upfield, indicating interactions between the 4AP protons, silver nanoparticles, and the CD cavity environment. These spectral changes confirm that 4AP effectively interacts with both the silver nano surface and CD interior, supporting the formation of stable inclusion-based nanomaterials.

Table 3. *^{1}H-NMR chemical shift values for the 4AP and Ag: 4AP: CD nanomaterials.*

Protons	4AP (δ)	A: 4AP: α-CD	Ag: 4AP: β-CD
H_A for OH	8.36	5.62	5.65
H_B ortho to OH	6.49	4.80	4.83
H_C meta to OH	6.43	3.61	3.65
H_D for NH_2	4.36	2.50	2.51

4. Conclusion

The spectral properties of 4-aminophenol (4AP) in the presence of α-CD and β-CD at pH ~2, pH ~7, and pH ~11 were investigated using UV-visible absorption, steady-state fluorescence, time-resolved fluorescence, and molecular modeling techniques. Ag: 4AP: CD nanomaterials were synthesized and characterized by SEM, DSC, FTIR, and Ⱨ NMR analyses. In aqueous solution (pH ~7), 4AP shows a blue-shifted absorption maximum and a red-shifted emission maximum compared with the other pH environments. While acidic conditions (pH ~2) induce a slight blue shift without major spectral changes, basic conditions (pH ~11) result in a noticeable red shift. At higher β-CD concentrations, the absorption spectrum of 4AP at pH ~7 becomes similar to that observed at pH ~2. Increasing CD concentration leads to dual emission in the excited state.

Changes in emission intensity at pH ~7 and the structured emission profile observed at pH ~11 indicate that 4AP forms excimers in the excited state; however, dimer formation does not occur in the ground state because the amino and hydroxyl groups are ionized. Lifetime measurements further demonstrate that the β-CD: 4AP inclusion complex is more stable than the α-CD complex. The molecular dimensions of 4AP allow complete encapsulation within both α-CD and β-CD cavities.

SEM-EDX analysis confirms that the nanomaterials contain 40.4% carbon, 50.4% oxygen, and 9.2% silver. Complementary characterization techniques—DSC, FTIR, XRD, and Ⱨ NMR—collectively support the successful formation of Ag: 4AP: CD nanomaterials.

Abbreviations

FTIR	Fourier Transform Infrared Spectroscopy
DTA	Differential Thermal Analysis
XRD	X-ray Diffraction
SEM	Scanning Electron Microscopy
HOMO	Highest Occupied Molecular Orbital
LUMO	Lowest Unoccupied Molecular Orbital

4AP	4-aminophenol
Ag NPs	Silver Nanoparticles
α-CD	Alpha Cyclodextrin
β-CD	Beta Cyclodextrin
PM3	Parametric Method 3
ΔE	Iinternal Energy Change
ΔH	Enthalpy Change
ΔG	Free Energy Change
ΔS	Entropy Change

Author Contributions

Narayanasamy Rajendiran: Supervision, Resources, Methodology, Software, Writing – original draft, Writing – review & editing

Ayyadurai Mani: Formal Analysis, Investigation

Palanichamy Ramasamy: Data curation

Sengamalai Senthilmurugan: Validation

Conflicts of Interest

The authors declare no conflict of interest.

References

[1] S. Menuel, J.-P. Joly, B. Courcot, J. Elysée, N.-E. Ghermani, A. Marsua, Synthesis and inclusion ability of a bis-β-cyclodextrin pseudo-cryptand towards Busulfan anticancer agent, Tetrahedron 67 (2010) 1706-1714. https://doi.org/10.1016/j.tet.2010.01.004

[2] T. R. Thatiparti, A. J. Shoffstall, H. A. von Recum, Cyclodextrin-based device coatings for affinity-based release of antibiotics, Biomaterials 31 (2010) 2335-2347. https://doi.org/10.1016/j.biomaterials.2009.11.061

[3] J. D. Artiss, K. Brogan, M. Brucal, M. Moghaddam, K. L. C. Jen, The effects of a new soluble dietary fiber on weight gain and selected blood parameters in rats. Metabolism 55 (2006) 195-202. https://doi.org/10.1016/j.metabol.2005.08.010

[4] G. Grunberger, J. D. Artiss, K. L. C. Jen, The benefits of early intervention in obese diabetic patients with FBCx™ - a new dietary fibre. Diabetes Metab. Res. Rev. 23 (2007) 56-62. https://doi.org/10.1002/dmrr.658

[5] P. Brocos, X. Banquy, N. Díaz-Vergara, S. Pérez-Casas, M. Costas, Á. Piñeiro, Similarities and differences between cyclodextrin-sodium dodecyl sulfate host-guest complexes of different stoichiometries: Molecular dynamics simulations at several temperatures. J. Phys. Chem. B 114 (2010) 12455-12467. https://doi.org/10.1021/jp103153h

[6] H. M. Ameen, S. Kunsági-Máté, L. Szente, B. Lemli, Encapsulation of sulfamethazine by native and randomly methylated β-cyclodextrins: The role of the dipole properties of guests. Spectrochim. Acta A 225 (2020) 117475. https://doi.org/10.1016/j.saa.2019.117475

[7] M. Jamróg iewicz, K. Milewska, Sacharides and their derivatives as pharmaceutical additives Spectrochim. Acta A 219 (2019) 346. https://doi.org/10.1016/j.saa.2019.04.033

[8] M. A. Chouker, H. Abdallah, A. Zeiz, M. H. El-Dakdouki, Host-guest inclusion complex of quinoxaline-1, 4-dioxide derivative with 2-hydroxypropyl-β-cyclodextrin: Preparation, characterization, and antibacterial activity. J. Mol. Struct. (2021) 130273. https://doi.org/10.1016/j.molstruc.2021.130273

[9] M. Levine, B. R. Smith, Tuning fluorescence energy transfer for carcinogen detection and medical diagnostics. J. Fluoresc. 30 (2020) 1015. https://doi.org/10.1007/s10895-020-02549-3

[10] I. Lafifi, L. Nouar, F. Madi, A. Guendouzi, M. Cheriet, N. Boulaha, B. Houari, Computational study of inclusion complex of L-Glutamine/β-Cyclodextrin: Electronic and intermolecular interactions investigations. J. Mol. Struct. 1206 (2020) 127740. https://doi.org/10.1016/j.molstruc.2020.127740

[11] M. Akhondi, E. Jamalizadeh, A. Mohebbi, MD and DFT calculations on the structural variations of amino-cyclodextrin as a pH-sensitive carrier for smart carriage and release of Doxorubicin. J. Mol. Struct. 1230 (2021) 129855. https://doi.org/10.1016/j.molstruc.2021.129855

[12] A. Obaid, A. Khairani, M. Jamil, S. Prabu, S. M. Saharin, S. Mohamad, Spectroscopic studies for the inclusion complexation of ketoprofen enantiomers with β-cyclodextrin. Spectrochim. Acta A 225 (2020) 118674. https://doi.org/10.1016/j.saa.2019.118674

[13] H. He, C. Xie, Y. Liu, N. Ge, Y. Wang, A fluorescent sensor for rapid and selective detection of Al (III) ions based on a naphthalimide-Schiff base derivative. J. Fluoresc. 31 (2021) 63. https://doi.org/10.1007/s10895-020-02652-5

[14] M. Ceborsk, Spectroscopic and structural investigation of ZnO nanoparticles prepared by microwave-hydrothermal method in the presence of ethylenediamine. J. Mol. Struct. 1165 (2018) 62. https://doi.org/10.1016/j.molstruc.2018.03.049

[15] L. Leclercq, H. Bricout, S. Tilloy, E. Monflier, Effect of cyclodextrin modification on inclusion complexation: the case of β-cyclodextrin and cholesterol. J. Colloid Interface Sci. 307 (2007) 481-487. https://doi.org/10.1016/j.jcis.2006.12.022

[16] R. K. Sankaranarayanan, A. Antony Muthu Prabhu, N. Rajendiran, Inclusion complexation of 3, 5-dihydroxy benzoic acid with β-CD at different pH. Indian J. Chemistry, 48A (2009) 1515-1521.

[17] R. K. Sankaranarayanan, A. Antony Muthu Prabhu, N. Rajendiran, A Study on the inclusion complexation of 3, 4, 5-trihydroxybenzoic acid with β-CD at different pH. J. Inclusion Phenomena and Macrocyclic Chemistry, 67(2010) 461-470, https://doi.org/10.1007/s10847-010-9765-3

[18] T. Stalin, P. Vasantharani, B. Shanthi, A. Sekar, N. Rajendiran, Inclusion complex of 1, 2, 3-trihydroxybenzene with α- and β-cyclodextrins. Indian J Chemistry, 45A (2006) 1113-1120.

[19] J. Prema Kumari, A. Antony Muthu Prabhu, G. Venkatesh, V. K. Subramanian, N. Rajendiran, Effect of solvents and pH on β-CD Inclusion complexation of 2, 4-dihydroxy azobenzene and 4-hydroxy azobenzene. J. Solution Chemistry, 40 (2011) 327-347. https://doi.org/10.1007/s10953-010-9713-3

[20] J. Prema Kumari, A. Antony Muthu Prabhu, G. Venkatesh, V. K. Subramanian, N. Rajendiran, Spectral characteristics of sulfadiazine, sulfisomidine: Effect of solvents, pH and β-CD. Physics and Chemistry of Liquids, 49(2011) 108-132. https://doi.org/10.1080/00319100903273372

[21] N. Rajendiran, R. K. Sankaranarayanan, Azo dye/Cyclodextrin: New findings of identical nanorods through 2: 2 inclusion complexes. Carbohydrate Polymers, 106 (2014) 422-431. https://doi.org/10.1016/j.carbpol.2014.02.042

[22] N. Rajendiran, R. K. Sankaranarayanan, J. Saravanan, A study of supramolecular host-guest interaction of dothiepin and doxepin drugs with cyclodextrin macrocycles. J Molecular Structure, 1067(2014) 252-260. https://doi.org/10.1016/j.molstruc.2014.03.034

[23] A. Antony Muthu Prabhu, N. Rajendiran, Encapsulation of labetalol, and pseudoephedrine in β-CD cavity: Spectral and molecular modeling studies. J. Fluorescence, 22(2012) 1461-1474. https://doi.org/10.1007/s10895-012-1053-5

[24] M. Jude Jenita, G. Venkatesh, V. K. Subramanian, N. Rajendiran, Twisted Intramolecular Charge Transfer effects on fast violet B and fast blue RR: Effect of HP-α-CD and HP-β-CDs. J. Molecular Liquids, 178 (2013) 160-167. https://doi.org/10.1016/j.molliq.2012.11.033

[25] N. Rajendiran, R. K. Sankaranarayanan, J. Saravanan, Nanochain and vesicles formed by inclusion complexation of 4, 4'-diamino benzanilide with Cyclodextrins. J. Experimental Nanoscience, 10(2015) 880-899. https://doi.org/10.1080/17458080.2014.930523

[26] A. Mani, P. Ramasamy, A. Antony Muthu Prabhu, N. Rajendiran, Investigation of Ag and Ag/Co bimetallic nanoparticles with naproxen-cyclodextrin inclusion complex. J. Molecular Structure, 1284 (2023) 135301-10. https://doi.org/10.1016/j.molstruc.2023.135301

[27] A. Mani, G. Venkatesh, P. Senthilraja, N. Rajendiran, Synthesis and Characterisation of Ag-Co-Venlafaxine-Cyclodextrin Nanorods, European J Advanced Chemistry Research, 5 (2024) 9-16. https://doi.org/10.24018/ejchem.2024.5.1.147

[28] A. Mani, P. Ramasamy, A. Antony Muthu Prabhu, P. Senthilraja, N. Rajendiran, Synthesis and Analysis of Ag/Olanzapine /Cyclodextrin and Ag/Co/Olanzapine /Cyclodextrin Inclusion Complex Nanorods. Physics and Chemistry of Liquids, 62 (2024) 196-209. https://doi.org/10.1080/00319104.2023.2297223

[29] A. Mani, P. Ramasamy, A. Antony Muthu Prabhu, P. Senthilraja, N. Rajendiran, Synthesis and Characterisation of Ag/Co/Chloroquine/Cyclodextrin Inclusion Complex Nanomaterials. J Sol-Gel Science and Technology 115 (2025) 844-856. https://doi.org/10.1007/s10971-024-06620-5

[30] N. Rajendiran, A. Mani, M. Venkatesan, B. Sneha, E. Nivetha, P. Senthilraja, Spectral, Microscopic, Antibacterial and Anticancer Activity of Pyrimethamine drug with Ag nano, DNA, RNA, BSA, Dendrimer, and Cyclodextrins, J Solution Chem, In press.

[31] S. Hamai, A. Hatamiya, Excimer formation in inclusion complexes of β-cyclodextrin with 1-alkylnaphthalenes in aqueous solutions. Bull. Chem. Soc. Jpn. 69 (1996) 2469-76. https://doi.org/10.1246/bcsj.69.2469

[32] S. Hamai, The excimer fluorescence of 2-methylnaphthalene in β- and γ-cyclodextrin aqueous solution. Bull. Chem. Soc. Jpn. 69 (1996) 543-549. https://doi.org/10.1246/bcsj.69.543

[33] S. Hamai, Cyclodextrin inclusion compounds. 1. Effects of β- and γ-cyclodextrins on the fluorescence of pyrene in aqueous solution. J. Phys. Chem. 93 (1989) 6527-29. https://doi.org/10.1021/j100346a037

[34] R. S. Sarpal, S. K. Dogra, Prototropism in aminophenols and anisidines: A reinvestigation. J. Photochem. 38 (1987) 263-276. https://doi.org/10.1016/0047-2670(87)85028-5

[35] N. Rajendiran, M. Swaminathan, Luminescence characteristics of 4, 4′-diaminodiphenyl methane in different solvents and at various pH. Spectrochim. Acta A 52 (1996) 1785-1792. https://doi.org/10.1016/0584-8539(96)01743-3

[36] T. Stalin, R. Anithadevi, N. Rajendiran, Spectral characteristics of ortho, meta and para dihydroxybenzenes in different solvents, pH and β-cyclodextrin. Spectrochim. Acta A 61 (2005) 2495 -510. https://doi.org/10.1016/j.saa.2004.03.030

[37] M. C. Rath, D. K. Palit, T. Mukherjee, Effects of organised media on the excited-state proton transfer in 2-(2′-pyridyl) benzimidazole. J. Chem. Soc. Faraday Trans. 94 (1998) 1189 - 93. https://doi.org/10.1039/A800017A

[38] S. Shaomin, et al., Study on inclusion interaction of piroxicam with β-cyclodextrin derivatives. Spectrochim. Acta A 59 (2003) 3379-86. https://doi.org/10.1016/S1386-1425(03)00078-3

[39] J. B. Chao, H. B. Tong, S. P. Huang, D. S. Lie, Preparation and study on the solid inclusion complex of sparfloxacin with β-cyclodextrin. Spectrochim. Acta A 60 (2004) 161-65. https://doi.org/10.1016/S1386-1425(03)00264-2

[40] P Ramasamy, A Mani, B Sneha, E Nivetha, M Venkatesan, N Rajendiran, Azo-hydrazo tautomerism in Sudan Red-B and Cyclodextrin/ Sudan Red-B doped ZnO nanomaterials. J Molecular Structure 1329 (2025) 141423-32. https://doi.org/10.1016/j.molstruc.2025.141423

[41] P. Ramasamy, A. Mani, B. Sneha, E. Nivetha, A. Antony Muthu Prabhu, G. Venkatesh, N. Rajendiran,* Synthesis and Characterisation of Sudan Red-G/Cyclodextrin doped ZnO Nanocrystals. American J Physical Chemistry 14 (2025) 23-32, https://doi.org/10.11648/j.ajpc.20251402.12

[42] P. Ramasamy, A. Mani, B. Sneha, E. Nivetha, A. Antony Muthu Prabhu, G. Venkatesh, P. Senthilraja, N. Rajendiran*, Synthesis and Characterisation of Cyclodextrin /Methyl Violet doped ZnO Nanocrystals. Colloid and Surface Science 9 (2025) 19-30, https://doi.org/10.11648/j.css.20250701.12

[43] P. Ramasamy, A. Mani, B. Sneha, E. Nivetha, A. Antony Muthu Prabhu, G. Venkatesh, P. Senthilraja, N. Rajendiran*, Synthesis and Characterisation of Cyclodextrin/ Sudan Black-B Caped ZnO/ Nanocrystals. American J Quantum Chemistry and Molecular Spectroscopy 9 (2025) 1-11, https://doi.org/10.11648/j.ajqcms.20250901.11

[44] P. Ramasamy, A. Mani, A. Antony Muthu Prabhu, G. Venkatesh, N. Rajendiran* Azo-Imino Tautomerism in Sudan Red 7B/Cyclodextrin Coated ZnO Nanocomposites: Evidence by Spectral and Microscopic Perspectives. Science Journal of Chemistry 13 (2025) 65 - 75, https://doi.org/10.11648/j.sjc.20251303.13

[45] P. Ramasamy, A. Mani, A. Antony Muthu Prabhu, G. Venkatesh, P. Senthilraja, N. Rajendiran* PICT Effects and Anticancer Potential on Rosaniline and Spectral Characterisation of Rosaniline/Cyclodextrin Covered ZnO/ Nanocrystals. International J. Pure and Applied Chemistry 26 (2025) 107-121, https://doi.org/10.9734/irjpac/2025/v26i3921

[46] P. Ramasamy, A. Mani, P. Senthilraja, N. Rajendiran Keto-Enol Tautomerism and Anticancer Potential on Sudan Blue II and Synthesis and Characterisation of Sudan Blue II/ Cyclodextrin doped ZnO Nanocrystals, J. Materials Science and Nanotechnology, 13 (2025) 1- 16.

[47] P. Ramasamy, A. Mani, P. Senthilraja, N. Rajendiran, Spectral, Microscopic and Anticancer Activity Investigation on Dimethyl Yellow/Cyclodextrin Doped ZnO Nanocomposites Journal of Chemical and Pharmaceutical Sciences (JCHPS) 18(3) (2025) 33-43.

[48] [P. Ramasamy, A. Mani, P. Senthilraja, N. Rajendiran, Spectral Characteristics of ZnO/Mordent Yellow 12/ Cyclodextrin Nanomaterials, J Chemical Health Risks, (JCHR) 15(2025) 542-553, ISSN: 2251-6727 www.jchr.org

[49] [P. Ramasamy, A. Mani, P. Senthilraja, S. Senthilmurugan, N. Rajendiran, Spectral, Microscopic and Anticancer Activity of 1, 8-Diaminonaphthalene Doped ZnO Nanocrystals, VVI-JOURNAL 14 (2026) 135-147, https://vvijournal.com/